EUROPEAN ORGANIZATION FOR NUCLEAR RESEARCH

CERN – PS-LP(CTF).NOTE 90-29

July 11, 1990

THE PROPOSED BEAM OPTICS FOR THE CLIC TEST FACILITY AND THE INSTRUMENTATION LAY – OUT.

A.J.Riche,CERN, PS

Abstract

A scheme for the CTF beam optics is given Fig 1. This extends from the RF – gun up to the CLIC beam transfer structure. This scheme is now fixed for the elements concerning all the instrumentation analysing the bunch of the RF gun.

Instrumentation is not the subject of this note, but is mentioned because, after the gun, the optics have been designed, in an iterative process, to optimize the lay – out of these instruments.

S. Battisti, M.Legras, P.Tetu, L.Thorndahl are the designers of the instrumentation.

The optics depend also on many mechanical aspects, including details for assembly, and lay – out of the vacuum scheme. As an example, the vacuum chamber and elements for measuring the beam should be baked (see Appendix 1). This decision changes the apertures chosen for the focusing elements and interferes with the possible choices for instrumentation, and is being followed up by J.C.Godot. P.Bossard has participated in the magnet specification. Their design is a compromise between rapid availability and ideal performance. Many suggestions made by J.Madsen has been incorporated into this study.

Content

Introduction.

The optics should guide the beam between the 4.5 MeV RF gun, the 60 MeV accelerating section and the structure used for transferring the energy from this drive linac to the CLIC accelerating structure.
In addition, the beam should also be shaped for going through available instruments.
The beam characteristics, are specified for the energy transfer required by CLIC [1],[2],[3],[4].
Mastering the fabrication of the photo−cathodes, the use of the laser ,of the RF gun, and if possible beam compression, requires a rapidly available set of instruments and corresponding beam optics.
However, when shifting along this long line of instruments, the bunch, which is not fully relativistic may loose its quality (see Appendix 2). After improvements, it is not excluded that an RF−gun would be placed directly at one end of the ACS. Up to now are foreseen, for the 4.5 MeV beam :

SEM−grids and screens for beam transverse images and possible use in emittance measurements.

Deflecting RF cavity for study of the longitudinal distribution in the bunch

UMAs and−or other type of monitors for measuring the beam charge and the beam centre position..

Faraday cup .

Spectrometer and slits associated with the spectrometer and with the deflecting RF cavities

Transition and Cerenkov radiation monitors also for the longitudinal distribution in the bunch, in association with a streak camera.

The optics here are calculated to a first order only, as the most important elements (quadrupoles, dipoles) do not exist yet, and the aberrations of the fields cannot be evaluated. Even space charge effects are not taken into account. The layout was established on the basis of calculations with TRANSPORT, and it is expected that, as at BNL, trimming all elements according to further higher order calculations will give good results, even for the highest charge we could produce, (charge at CERN is higher, but somewhat more diluted longitudinally).

Input beam characteristics.

For specifications of the series of bunches we refer to [1],[2],[3],[4]. A series of runs with program TBCISF and some with PRIAM [5], have established the correspondence between laser pulse and photocathodes characteristics with the parameters of the bunches at the RF−gun exit. Beam optics were simulated from parameters given as output by running TBCISF (Ref.:output by J.Stroede and H. Kugler)
'RF 184/9.4 nC/100 MV m − 1/ 30. ps/ 4 A mm − 2/ 30 deg
Corresponding beam parameters at the end of the RF−gun are given in Appendix 3.
Other input parameters for the optics were used to see if the focusing system could cope with larger emittance or beam divergence, but just as verification.
They correspond to different values of the RF/laser phase shift, radius of laser spot, pulse length, and amount of emitted charge.

From the first experience to fulfillment of the beam specifications, the characteristics of the beam will differ considerably: a tentative of description of the different stages is given in Appendix 4.

Principle: Permanent use of a spectrometer.

We have adopted the solution chosen by BNL [6] for similar reasons:
The lay−out results from 2 deliberate choices:
a) a 90 deg. sector magnet as a spectrometer.
b) the permanent use of this spectrometer.
As a consequence, a dispersion suppressor is necessary, involving a second sector magnet and 2 focusing quadrupoles.
The system has several interesting features:

- possible illumination of the photocathode by a laser beam on axis,
- possibility of a permanent restriction of the momentum acceptance by the slits, with correlated effect of cutting the bunch length.
- availability of free drifts associated with the spectrometer system for housing instruments where transverse beam extent is small.
- economy of longitudinal dimension with a beam returning back after 2 times 90 deg. bend.
- Availability ,if the current in the second bend is off, of further beam line for experiment.

Instrumentation.

The spectrometer and its front focusing .

Focusing.

The focusing properties of sector magnet are well known: a beam having a horizontal waist at a distance d in front of the magnet entry face has again another waist at D after the exit face. The principle is illustrated on Fig. 2. and 3. To first approximation, the segment joining the object and image passes by the edge of the sector magnet.
A slit is placed at the second waist where there is dispersion. There, the transverse size of the beam, due to pure emittance (mono chromatic beam), is small compared to the size due to the momentum dispersion. The transverse distribution is then dominated by the transverse size due to the energy spectrum, not by the beam size resulting from the pure emittance, the figure of merit being

$\frac{D_x \frac{dp}{p}}{\sigma_x}$ where D_x is the dispersion, $\frac{dp}{p}$ one standard deviation of the momentum spread, and σ_x the standard deviation for the horizontal beam projection. supposing the beam monochromatic. With the lay−out we have selected:

```
sigmax  (m) = .109
D       (m) = .6
dp/p        = .045
```

Dispersion enclosed between the 2 bendings.

2 focusing quadrupoles are adjusted to achieve the suppression of the dispersion after the second bend. Between them, the dispersion is maximum: it is the place for the vertical slit.

Between the quadrupole and the second bending, we measure the bunch charge and, when slits are open, the position of the beam centre, but with dispersion (I.P type UMA monitor forseen).
The strength of these quadrupoles is related to the geometry: Once the dipoles are specified, and for a given central momentum, we have a correlation between the gradient in the quadrupoles, and the distances: λ , between the quadrupoles and the dipoles, d, between the quadrupoles, l, the length of the quadrupoles.
This is shown on Fig.4 : If dipoles have their fields parallel, the choice of d is free, the quadrupole strength is chosen according to the space λ required for housing the UMA.
As shown also on Fig.4, if fields are anti parallel, the strength of the quadrupoles is too high, the resulting cell is far less transparent to incoming beam than with parallel fields.
Fig. 5 gives the relation between the dispersion D (m), the gradient and the lengths. For D = 0.6m, and l = 0.1m, we read a gradient of 0.15 T m − 1 , and a distance λ = 0.4 m .

Necessary focusing in front of the sector magnet.
Despite the large beam divergence expected at gun exit, 3 quadrupoles with large aperture, short length, but not necessarily high strength would provide necessary high β x, low β x succession in front of the 90 degrees sector magnet.
Because of lack of time for magnet design and construction, we try to use LILV − type quadrupoles. By re − shaping the poles to get 80 mm bore instead of original 58 mm, we could use a 60 mm inner diameter chamber, allowing $\pm$ 2 σ for the beam transverse extent.
Because our quadrupoles are not short enough, we need the focusing strength of a solenoid in front of the quadrupoles.
The net effect is focusing in both transverse planes: beam size is small just in front of the bending magnet, we can place there the RF deflector. Its iris size (21 mm) copes with the 2 σ of the beam transverse size there.
The horizontal and vertical envelopes are plotted on Fig.6, 7 and 8 for the beam between RF gun and first dipole, and between the 2 dipoles.

Bunch length, and possible correlation between momentum and distance to bunch centre: RF transverse deflection.

The RF deflection turns the bunch such that it has an important transverse projection (vertical). To obtain the separation, we should use preferably the part of the RF pulse which is not too much non linear, and the highest peak voltage compatible with other constraints. The horizontal slits are placed where the betatron phase difference is suitable: between the quadrupoles , just after the vertical slits used for selecting a momentum bite, but closer to the second quadrupole.
A shift on the RF phase of the deflector is used just as is used the shift of the field in the bending magnet for the spectrometer: it selects different bites of the longitudinal distribution along the bunch, because of the vertical deflection.
The figure of merit (betatronic) is the ratio between a vertical displacement at the slit compared to an angular deviation at the centre of the deflector. For 1 mrad vertical deviation at the centre of the deflector, we have 1.4 mm beam displacement just between the 2 quadrupoles, and 1.8 mm in front of the second quadrupole.
With this arrangement, the same charge detector is used for the spectrometer and for the deflecting cavity.

The correlation between the distance from the particle to the centre of the bunch and the particle momentum could be measured if the detector sensitivity and RF slicing device were adequate, by having both slits and the RF deflecting structure operated at the same time.

Bunch length, distribution along the length by observing the Transition or the Cerenkov radiation.
Both measurements will be used for studies of the structure of the bunch in time .Good resolution requires small beam size, so the position between the first dipole and the following quadrupole is appropriate. It is also not too far from the gun(Appendix 2.)
This measurement will give the effect of the bunch compression which we intend to have after (60 MeV) or in front of the ACS.

Beam observation for steering optics
Unavoidable misalignments will be corrected by very short H and V dipoles (appendix 6). For verification of the focusing and also the steering, observation is forseen as follows:

Beam after gun
A SEM grid placed after the quadrupoles will help setting the 4 parameters of the focusing (solenoid and 3 quadrupoles). It will have wires with small diameter compared to their distances. The laser forbids using a screen.
Between this SEM grid and the deflecting structure, there is place for a UMA, giving precisely the beam centre transverse position and the charge.

Beam between the dipoles, or on the same line.
The Transition/Cerenkov monitors, the slits,the UMA occupy all the available space. Beam profile could be observed on a screen following the second bending, in the line behind the second magnet if it were switched off, but the dispersion will be present. A retractable screen allows the use of other experimental facilities at this place, as done at BNL: a Faraday cup.
Fig.9 gives the envelopes from the first sector magnet to the Faraday cup, when the second sector magnet, the 2 dispersion suppressors quadrupoles are at zero current. The place is less suitable than the mid−magnet point for setting the slit of the spectrometer.

after the second bending
Beam position and transverse extent should be observable at least at the entrance of the accelerating sections, the transfer structure, and at each group of quadrupoles, if possible.
Fig.10 gives the envelope from the gun to CLIC accelerating structure used as transfer structure, for a monochromatic beam. The distance between the accelerating structure and the second dipole is there a minimum chosen for easy focusing. The aperture of the CLIC accelerating structure is 4 mm diameter: it can be seen that the transverse dimension of the bunch can be well adapted to it.

Acknowledgments.
Particular thanks are due to K. Batchelor, of BNL, and to his colleagues, for advices, explanations, communications of papers. I thank also K.Hubner for reading the manuscript and commenting.

References:

1.Optimized Drive Bunches for a Two – Stage RF Linear Collider
W.Schnell, CERN/LEP – RF 86 – 14
2.A CLIC Injector Test Facility,
Y. Baconnier,K. Geissler, K.Hubner, J.H.B.Madsen,CLIC Note 65,June 88
3.The study of a CERN Linear Collider, CLIC
W.Schnell, CERN/LEP – RF 88 – 48, Linac 88
4.Minutes of the CLIC meeting ,Dec. 15 1989,CLIC – 42/BZ/ps,Dec20,1989
5.Beam Dynamics Simulations of the RF – gun, particle source of the CLIC Test Facility.
H.Kugler,A.Pisent,A.J.Riche,J.Stroede, EPAC 90, Nice
6.The Brookhaven Accelerator Test Facility. K.Batchelor, T.S.Chou,
J.Fisher, J.Gallardo, H.G.Kirk, R.Koul, R.B.Palmer, C.Pellegrini,
T.Srinivasan – Rao, S.Ulc,M.Woodle, BNL ; I.Biglio, N.Kurnit, LNL;
and K.T.McDonald, Princeton, Linac Conference 1988, Vancouver.
7.Resume de la reunion du 2 – 07 – 90 sur l' instrumentation du CTF
J.P.Potier, A.Riche, PS – LP(CTF) Note 90 – 31
8.A 0.2 m, 90 deg. sector – C Magnet for energy analysis on the CTF,
A.Riche, PS – LP(CTF) Note 90 – 17
9.Design data sheet for beam transport magnets, P.Bossart, 8 – 5 – 90
10.Specifications for construction of magnets for the CTF beam line
J.C. Godot.J.H.B.Madsen, A.Riche
11.Quadrupoles or solenoids for the CTF and the 2 bending system,A.Riche
12.Request to purchase LIL – type quadrupoles,
J.P.Delahaye,K.Hubner,J.H.B.Madsen, Memo 5/06/90
13.Request to purchase power supplies,
J.P.Delahaye,K.Hubner,J.H.B.Madsen, Memo 5/06/90
14.Photo – cathodes pour le CTF, Propositions preliminaires.
G.Suberlucq, PS/LP(CTF) 90 – 30 (en preparation)
15.Dipoles de correction pour le CTF. A.Riche,PS/LP(CTF) 90 – 32

Appendix 1:Remarks about the vacuum Baking at 150 deg.(possibility 300 deg.) is forseen (conf. J.C. Godot) We investigate the possibility of using a thin window to isolate ultra high vacuum needed for the alkaline photocathodes (1.E – 12 torr) from standard vacuum (1.E – 8 torr).

For the multiple Coulomb scattering, the non projected (space), or projected (plane) distributions are given by the gaussian forms:

$$f(\theta_{space})d\Omega = \frac{1}{\pi\theta_0^2}\exp - \frac{\theta^2_{space}}{\theta_0^2}\ d\Omega \quad \text{, and,} \quad g(\theta_{plane})d\theta_{plane} = \frac{1}{\sqrt{\pi}\theta_0}\exp - \frac{\theta^2_{plane}}{\theta_0^2}\ d\theta_{plane}$$

$$\text{with } \theta_0 = \frac{20}{p\beta}\sqrt{\frac{L}{L_r}}\left(1 + 0.111\ \log_{10}\frac{L}{L_r}\right)$$

For stainless steel, we take the same characteristics as for iron: radiation length L_r = 1.76 cm,

p= 4.5 MeV, and θ_e radians, we have:
with 25 E-6 m : θ_e = .11 rad = 6.5 deg.,
with 15 E-6 m : θ_e = 0.084 rad.

We abandon this solution because of the increase in emittance.

Appendix 2: Shifts of particles in non relativistic bunches.

dz = z dv/v

$d\beta / \beta = (1 / \gamma^2)(d\beta\gamma / \beta\gamma)$

then, dz = z (1/64) (1/100) for 4.5 MeV, and dp/p = 1. E−2

that is nearly 0.2 mm m−1 , which is not negligible for a bunch of less than 10 mm length.

Appendix 3: Input beam characteristics. The 30 deg. phase angle was chosen as the best compromise for having at the exit of the RF gun:

a high transmission (over .97)
a low dp/p (4.5 E-02)
the highest momentum (4.5 MeV/c)
a short bunch (1.8 E-03 m)

The characteristics are detailed below, with units m and MeV, if not otherwise specified. The emittance is defined as $\sqrt{(<u^2><u'^2> - <uu'>^2)}$

transverse projections on x (same results on y) and dx/ds		longitudinal projections on z and dp/p	
momentum		4.5	
sigmax	.049	sigmaz	1.8E-3
sigmadx/ds	.031	sigmadp/p	4.5E-02
emittance	4.5E-06		7.E-06
alpha	-34.53		0.48
beta	5.35		0.447
angle (deg) from x axis to ellipse main axis		from z axis	
81.2		101.3	

Appendix 4. Successive steps for experimenting the beam of the CTF Details about instrumentation were recently discussed in a meeting, on the 2−07−90. The minutes will be published, with full details [7]. The following paragraph only resumes the first proposals which were necessary to adapt beam optics to instrumentation.

Expected characteristics of the beam and proposal for intermediate instrumentation (information about lasers and photocathodes was supplied by K.Geissler and G.Suberlucq [14])

Constant :

RF frequency	3 GHz
duration of klystron input power	1 micro s
repetition rate	5 Hz
momentum	4.5 MeV

1. First experiment with dark current
   Intensity < 0.1 mA
   modulation following RF,
   energy peak 4.5 MeV (most particles coming from near the cathode)
   At first (September 89) intensity could be measured by photo-multiplier observing a screen, and energy by absorption.
   At BNL, a neutron detector was used, because the threshold for neutron production is close to the maximum energy.

2. Metallic cathode and long pulse laser illumination
   laser Nd YAG , commercially available, installed end 90 ?
   laser pulse length 5 ns
   wave length 266 nm
   power 3 mJ
   metallic cathode, quantum efficiency : 1.E-04 to 5.0E-04
   (if transported in vacuum)
   Modulation by the RF,as for the black current.
   Supposing 1 mJ , we get :
   5 E+12 * 266 * 1= 1.33 E+15 photons
   A laser pulse of 5 ns represents 15 periods at 3 GHz
   Per RF period, this gives 0.090 E+15 photons

	N e- per period at the cathode	N e- per period at gun exit	nC
minimum:			
1 mJ, Rq = 1.E-04	.9 E+10	in 180 deg .45 E+10	0.7
		in 36 deg .09 E+10	0.14
maximum:			
3 mJ, Rq = 5.E-04	13. E+10	in 180 deg 6.6 E+10	10.6
		in 36 deg 1.3 E+10	2.1

What is mentioned ' in 36 deg' represents the number of electrons per RF period, with spectrum cut by the conjugate effect of spectrometer and associated slit.

It is hoped that a correlation longitudinal distribution/energy will also help to get short bunches.
Bunches will be separated by 10 cm.

3.Laser specially designed for CTF :repetition rate 5 to 10 Hz
diode laser + crystal, 262 nm, synchronous with RF (May 91 ?)
metallic cathode (1.0 E-04 < Rq < 5.0 E-04), each pulse : 0.2 mJ
5 E+12 * 266 * 0.2 2.66 E+14 photons
the laser pulse length is 5 ps.

	N e- per period at the cathode	N e- per period at gun exit	nC
minimum: Rq = 1.E-04	2.7 E+10	2.7 E+10	4.3
maximum: Rq = 5.E-04	13.5 E+10	13.5 E+10	21

The laser is synchronous with the RF, the charge per pulse is identical in UMA235 and at gun exit. The bunch length is less than 1 cm, before compression. The repetition rate is according to the 30 GHz of the transfer structure. Simultaneous use of the slits associated with the spectrometer and with RF deflection should be possible.

4.High quantum efficiency alkaline cathodes (from July 91)
upper limit of expected quantum efficiency :
minimum 5.0E-03
minimum 5.0 E-03; maximum 5.0E-02 to 8.0E-02, but decreasing with time
some ten hours life time
It is considered that the maximum charge transmitted by the RF-gun is 50 nC, i.e. 30 E+10 e- per pulse.
This number will fall with time, with cathode ageing. The cathodes will be changed accordingly.

Filling the CLIC structure :
length of train < 12 ns filling time of the CLIC structure, which will be used in place of the real transfer structure, for which this time is 3 ns.

Tentative of specification for the measurement of the charge behind the slits:

a. Dark current will be measured, as soon as the gun is powered over 40 MV m-1, and,when possible, the spectrum will be measured (BNL).
b. The sensitivity should be such that it allows measuring the charge when the spectrometer slit, or the slit associated with the RF vertical deflection transmits only 1/10 of the bunch charge, if total charge is less than 1 nC.
c. For bunch charge of 1 nC or greater, simultaneous operation of both slits and measurements of the charge (1/100) should be possible.

Appendix 5: Magnets.

Beam transverse dimensions and vacuum chamber.

Ideal vacuum chamber clearance is 3 σ from the transverse dimensions of the beam, but we will only have 2 σ.

a. some 5 mm should be added to the external chamber radius to house the material used for baking and its isolation.

b. Quadrupoles similar to those of LILV are convenient for focusing in the last straight line, in front of the accelerating LIL section and of the transfer structure.

Behind the gun and just after the second dipole, the aperture of these quadrupoles is too small (58 mm), and their length too high.

Quadrupoles.

Constructing new magnets would have taken too much time. It was decided to specify these magnets as 'special versions' of the standard ones for the purchase, although these modifications are important (aperture increased from 58 mm to 80 mm, length of the iron core decreased by 1/3 for 3 quadrupoles following the second sector magnet.

Compromise : use a solenoid in front of the first quadrupole and allow only clearance for 2 σ of the transverse dimension of the beam. This leads to a vacuum chamber inner diameter of 60 mm after the gun.

Fig. 11 shows that the core of LILV quadrupoles are machined, and a new profile obtained, accepting the new dimensions of the chamber (diameter 61/63 mm). The section of the coil stays the same. The low field in the core allows the flux increase.

Dipoles.

Straight edges ideal field: For a trajectory of length .2 m in the dipole, the radius is .127 m, and the field: .12 T

Focusing effect would be ruined if the stray field were too important. We choose 51 mm for the gap, housing the 40.5/44.5 vacuum chamber, the system for baking and associated isolation. With this gap, the importance of the stray field stays small, as shown on Fig.12.

Because of the effect of the stray field, the field required will be 0.1 T, the trajectory will be , under the poles, very close to a circle of .151 m, with a centre at .035 m from the edge of the sector, as shown on Fig.13. Shims laid on the poles along the chamber will correct the field inhomogeneity, shims on the front and rear face of the magnet could be used for getting better definition of BL, if necessary, as shown on Fig.14.

Appendix 6: Correcting dipoles

In the first meters after the RFgun, the space is very limited for installing correcting dipoles. Then, simple rectangular iron frame dipoles are proposed,Fig.15, which can be installed over the vacuum chambers, when 3 cm space along the beam are available. [15]

Two types of dipoles are proposed, one type for the 60/63 mm vacuum chamber (on beam line nb 1, and on part of beam line nb 3), another type adapted for the 40/44 mm vacuum chamber (beam line nb 2, between the sector magnets, and beam line nb 3, after the reduction of the vacuum chamber diameter to 40/44 mm.

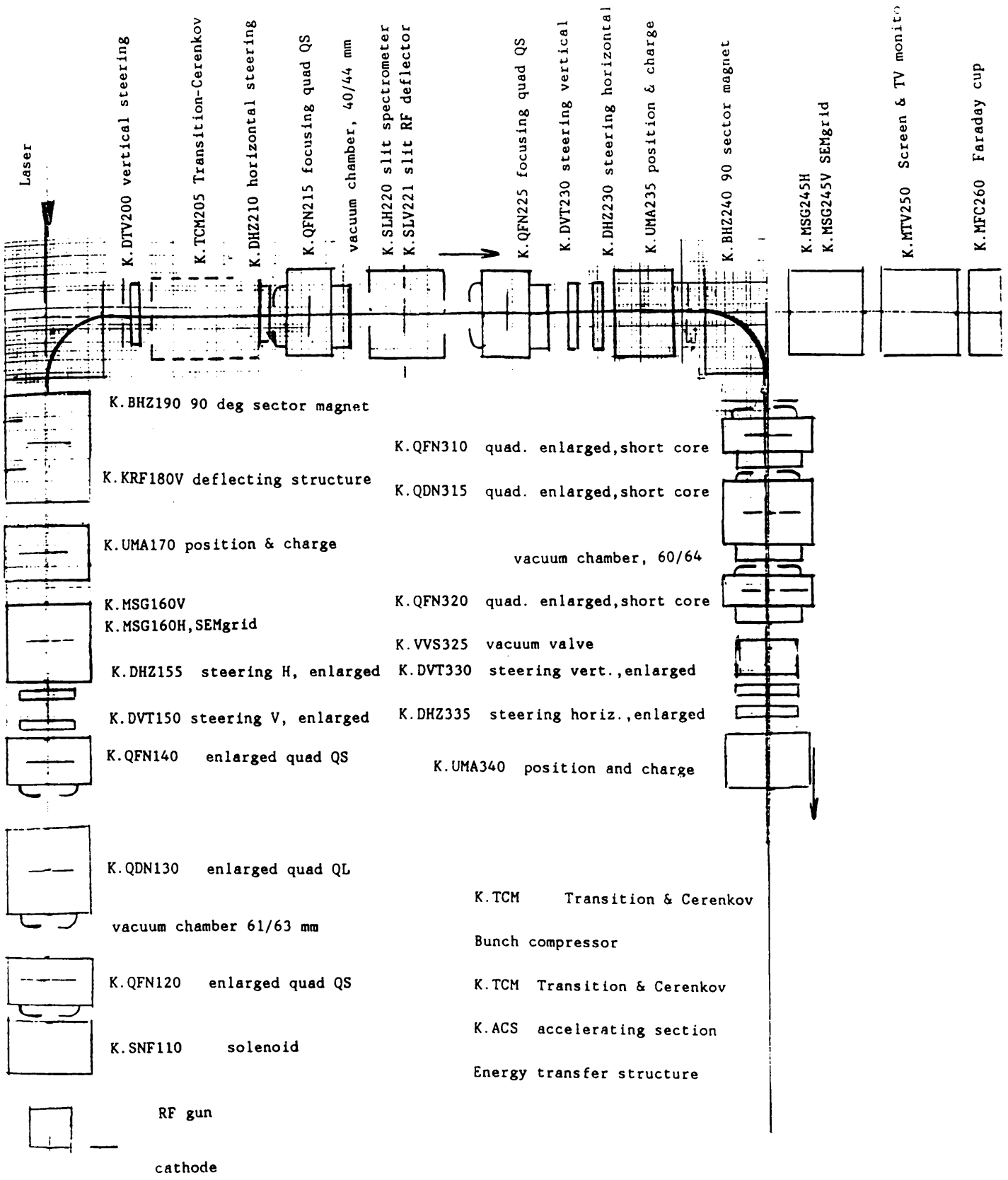

FIG 1 LAY-OUT FOR OPTICS AND INSTRUMENTATION
ON THE FIRTST 5 M OF CTF BEAM

Fig.2 Horizontal focusing effect by a 90 deg. sector magnet

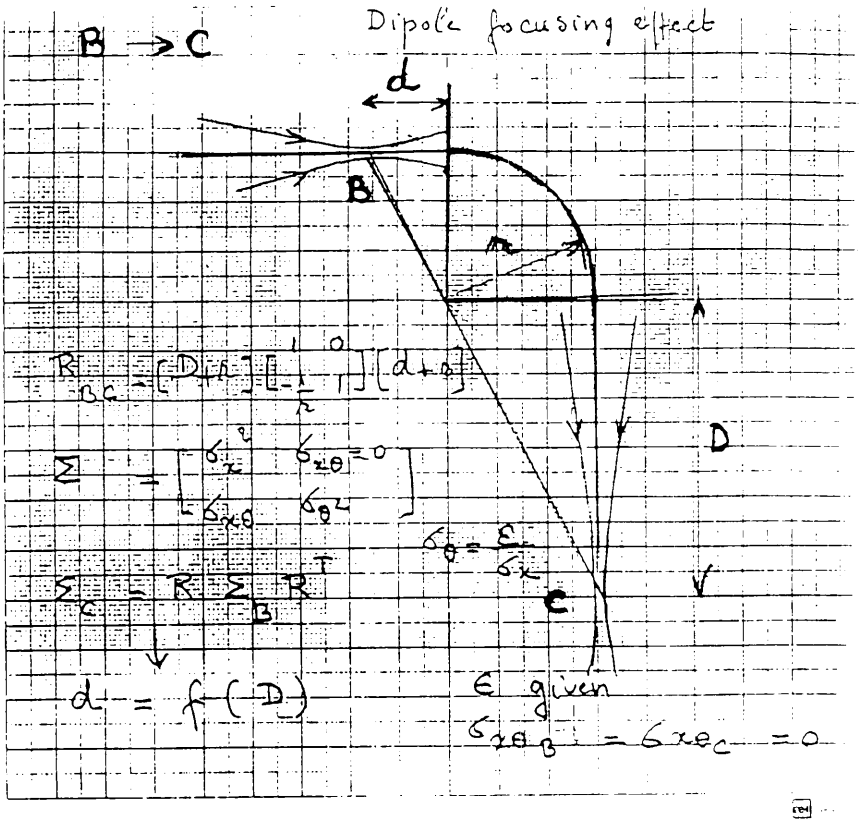

Fig.3 Focusing effects by the 90 deg sector dipole:
The 2 waists of the horizontal beam envelope

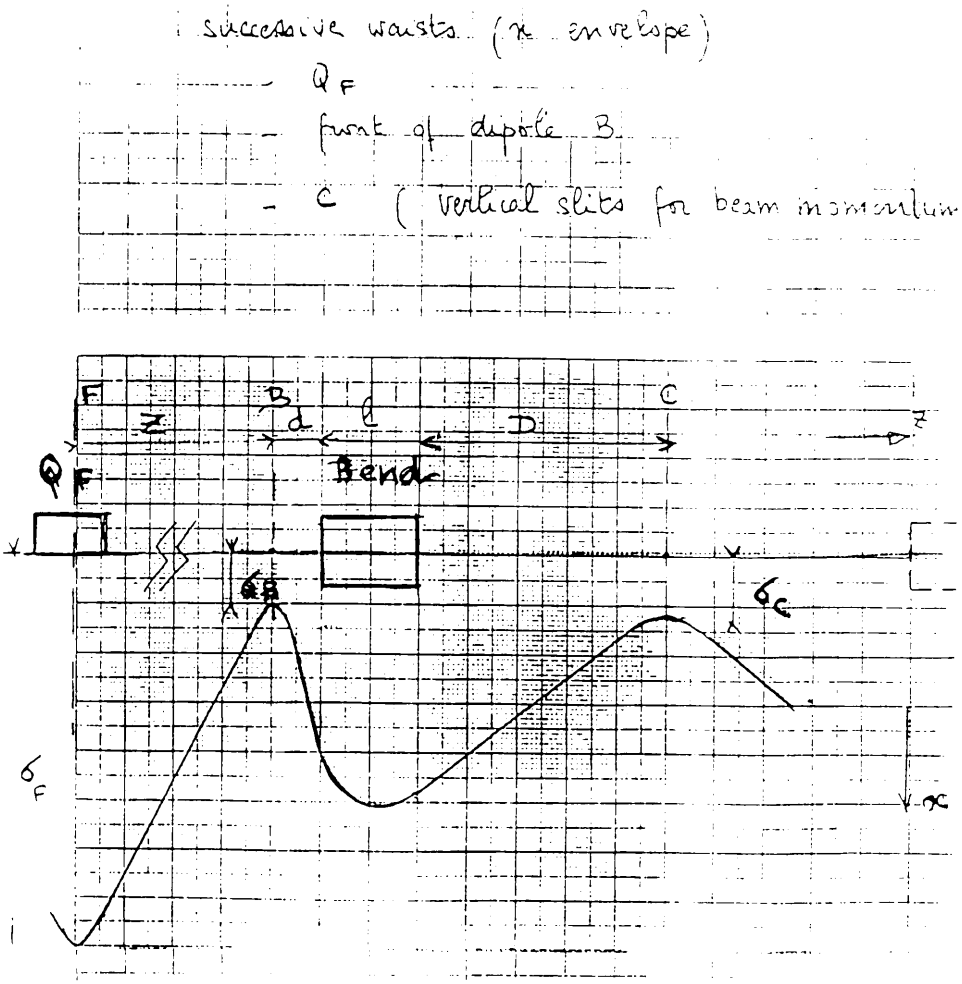

Fig.4 Distance dipole/quadrupole as function of gradient and distance between the quadrupoles for quadrupole length l= 0.1 m Bendings with parallel/opposite B

lambda is the distance between the quadrupole and the dipole

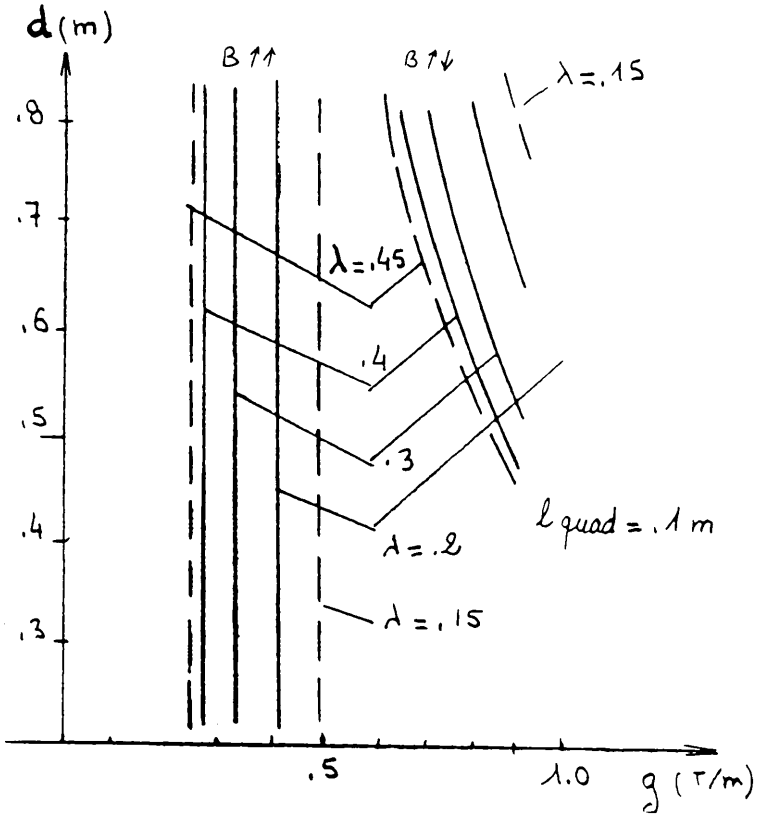

Fig.5 Dispersion and distance between quadrupole and dipole, as function of the gradient, for the cell with bendings with parallel B fields.

lambda is the distance between the quadrupole and the dipole, l the quadrupole length, D the dispersion.

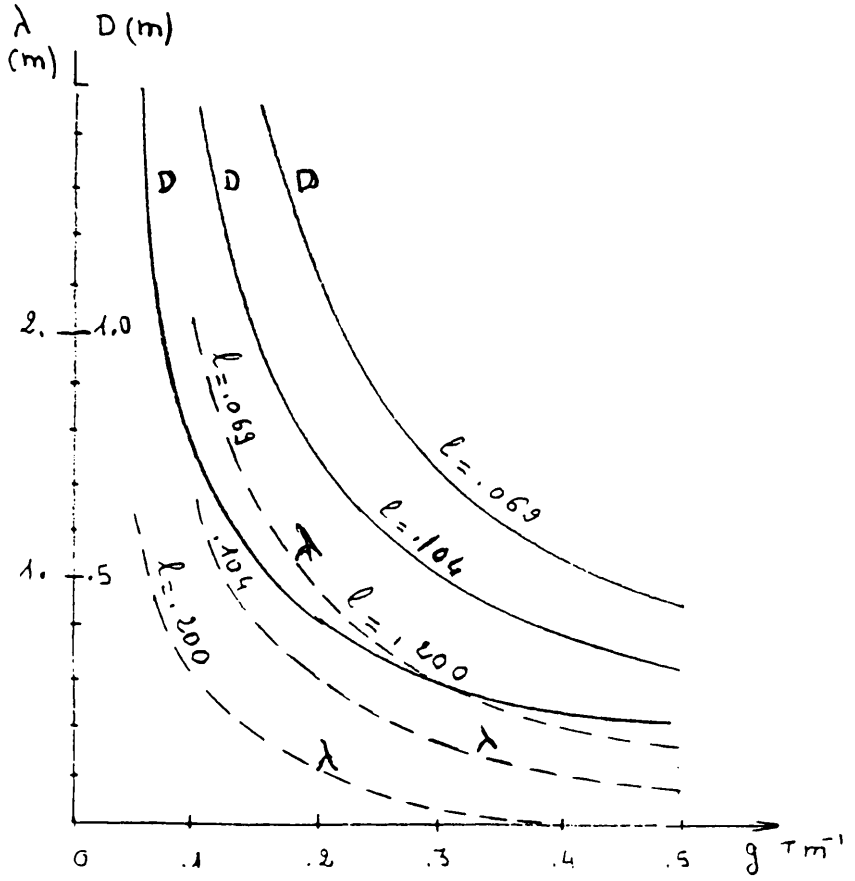

Fig.6 Horizontal and vertical envelopes from RF gun to the end of the 90 deg bending magnet, envelopes at 1 sigmax and 1 sigmay

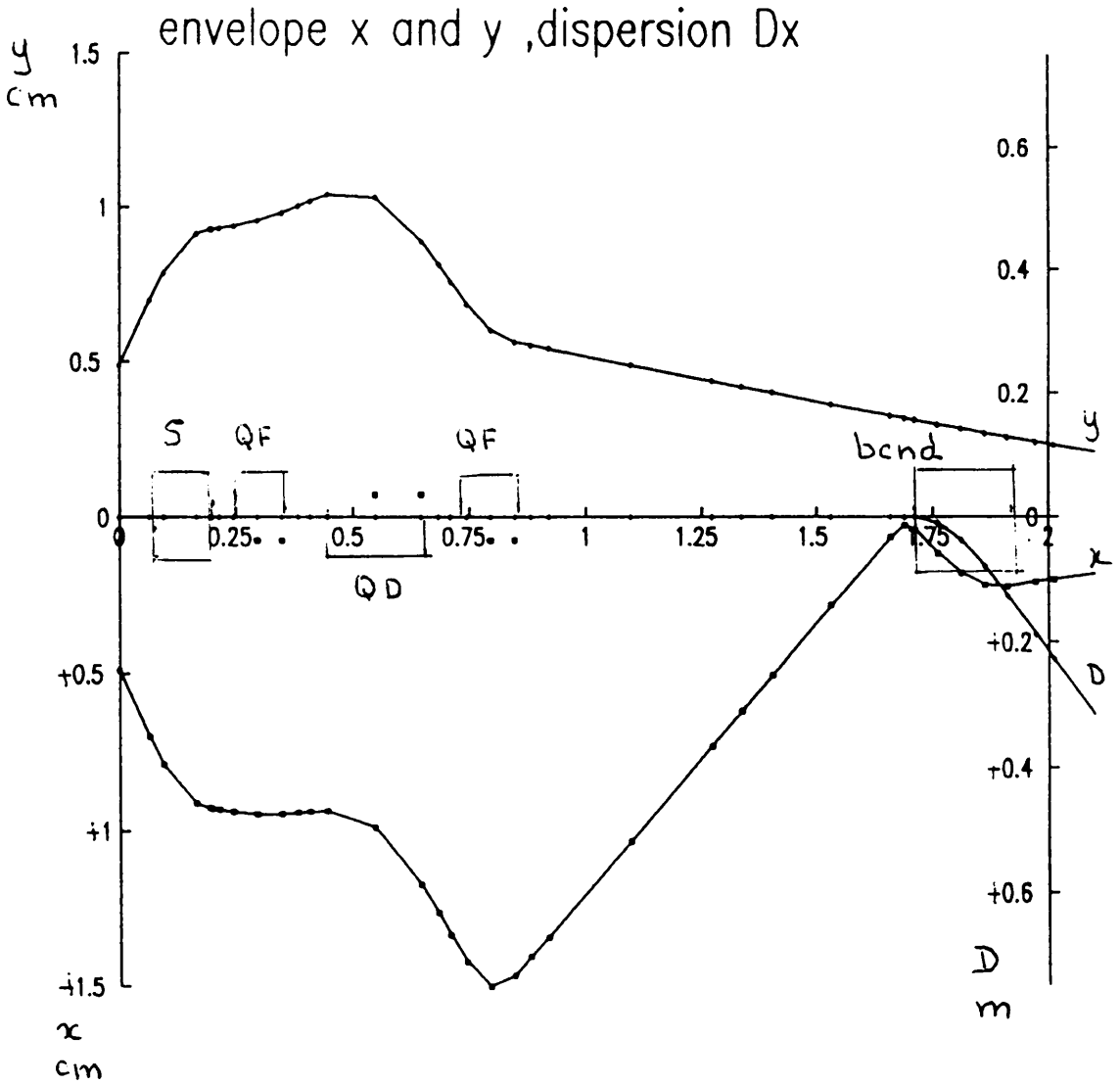

Fig.7 Horizontal and vertical beam envelope from RF gun to the end of the second bending monochromatic beam

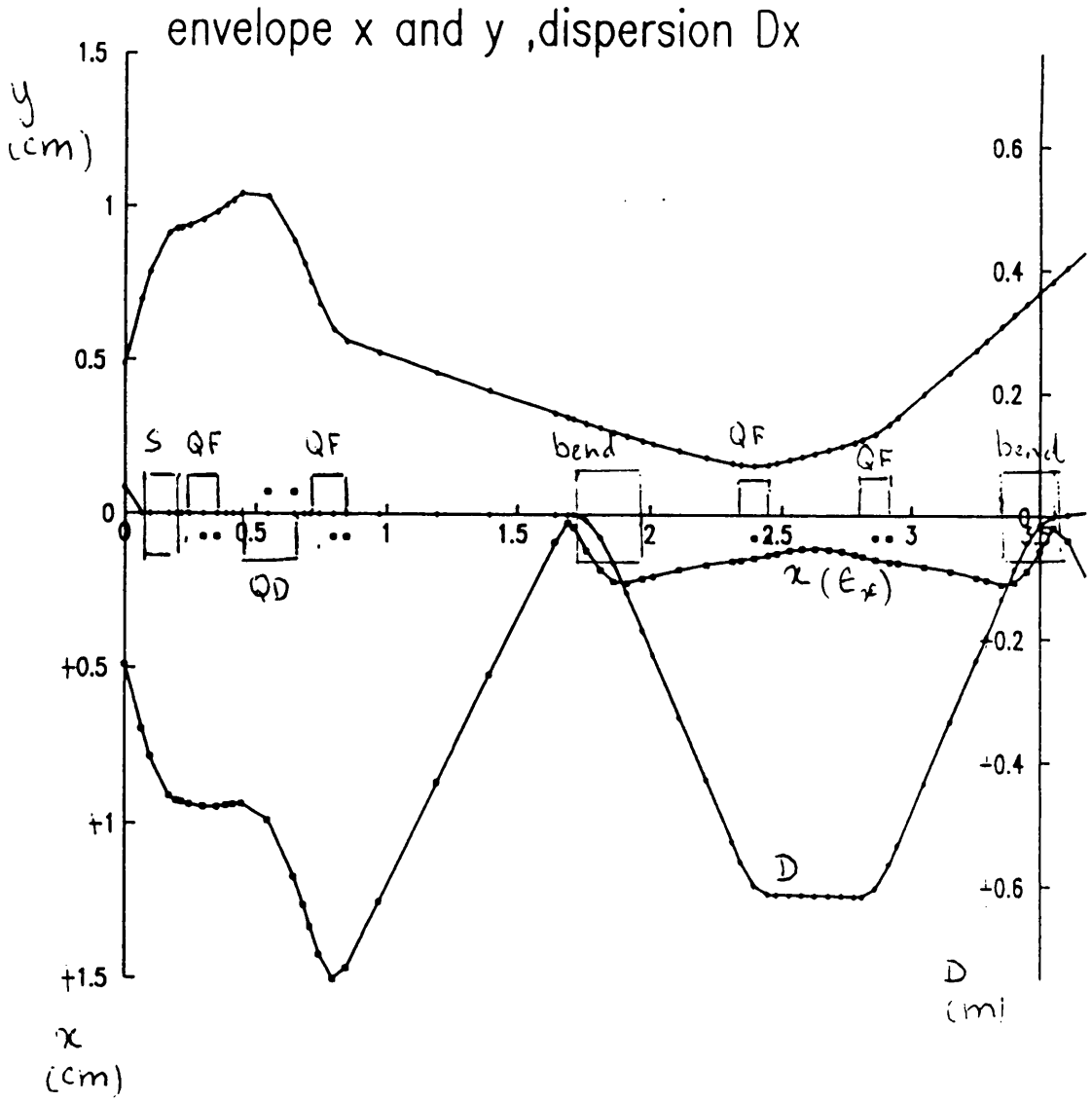

Fig.8 Horizontal and vertical beam envelope from RF gun to the end of the second bending beam with sigma dp/p = .045

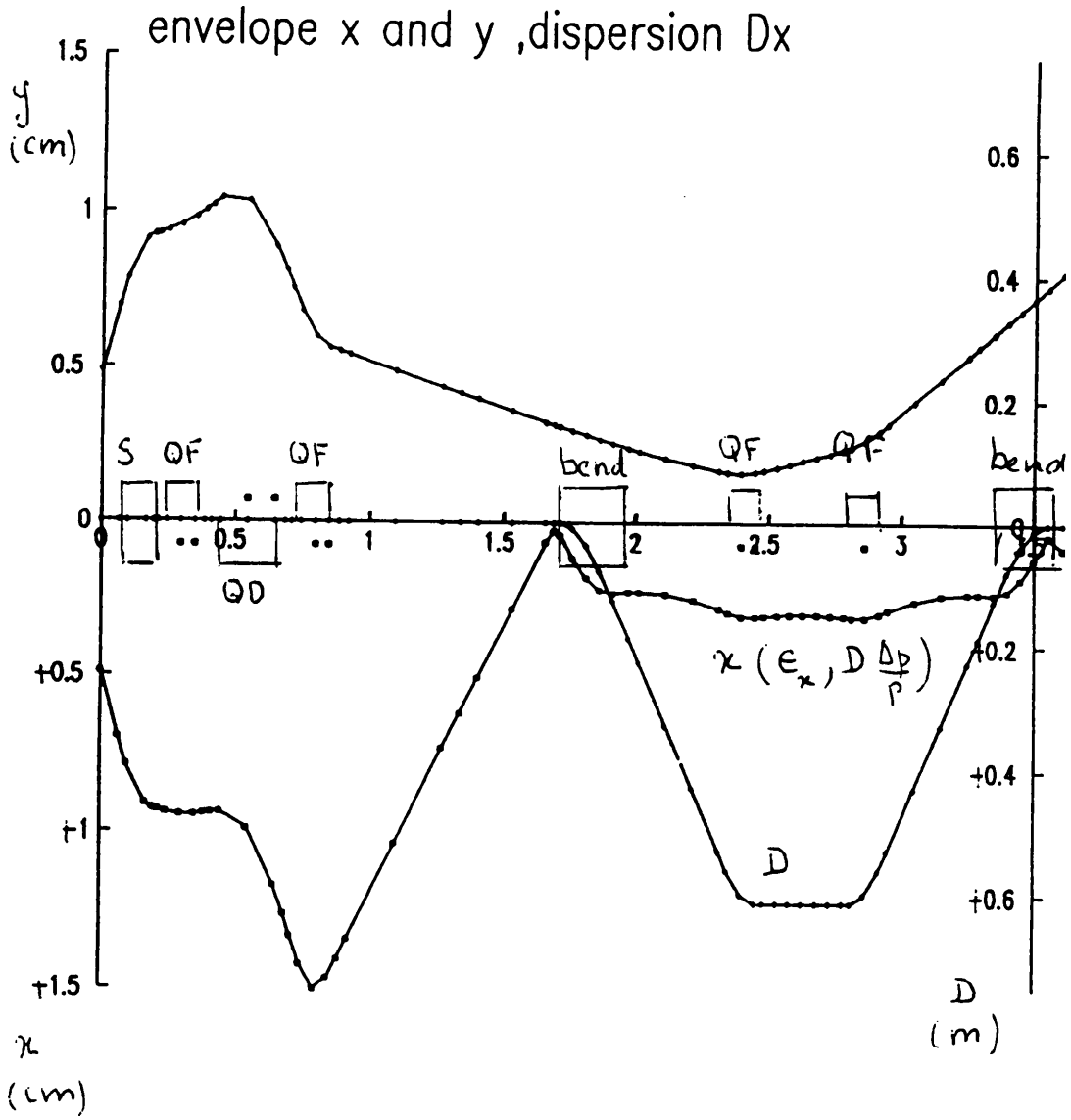

Fig.9 Horizontal and vertical beam envelope from RF gun to the end of the beam support nb 2 The 2 nd sector magnet and the 2 preceding quadrupoles are off.

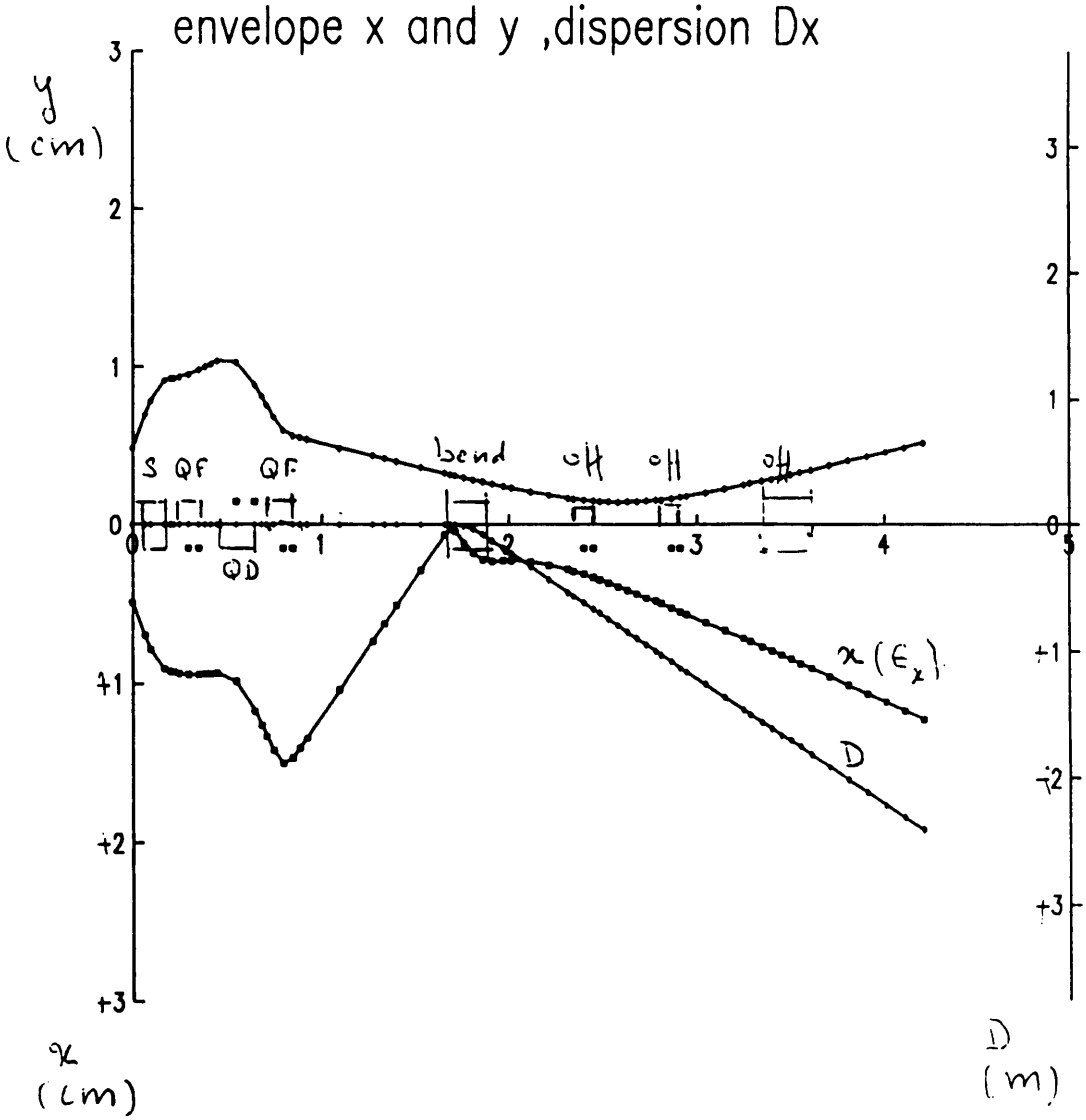

Fig. 10 Horizontal and vertical beam envelope from RF gun to the end of the CLIC power transfer structure. The envelopes are given at 1 sigma.

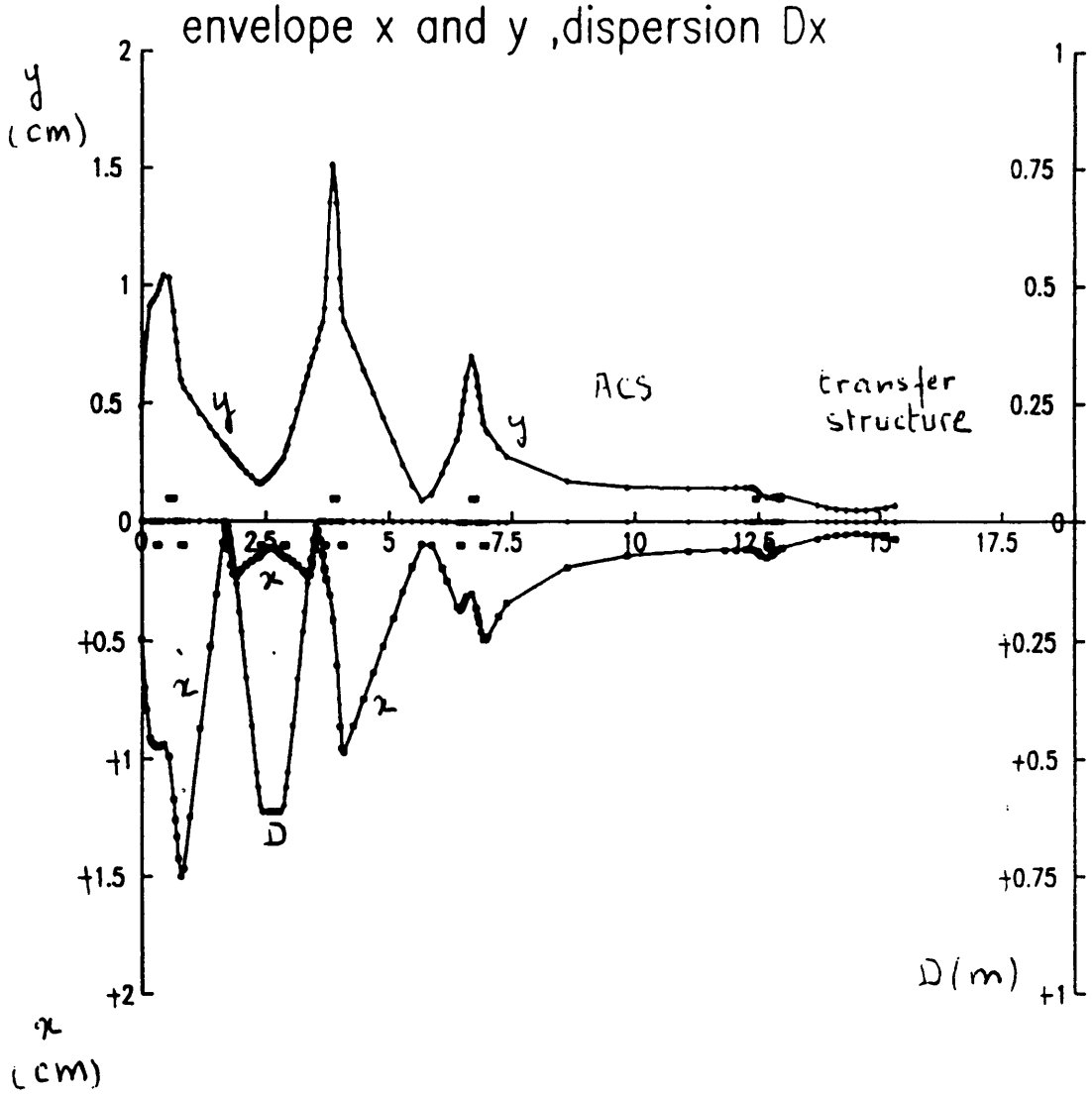

Fig.11 Present and modified quadrupole lamination and coill

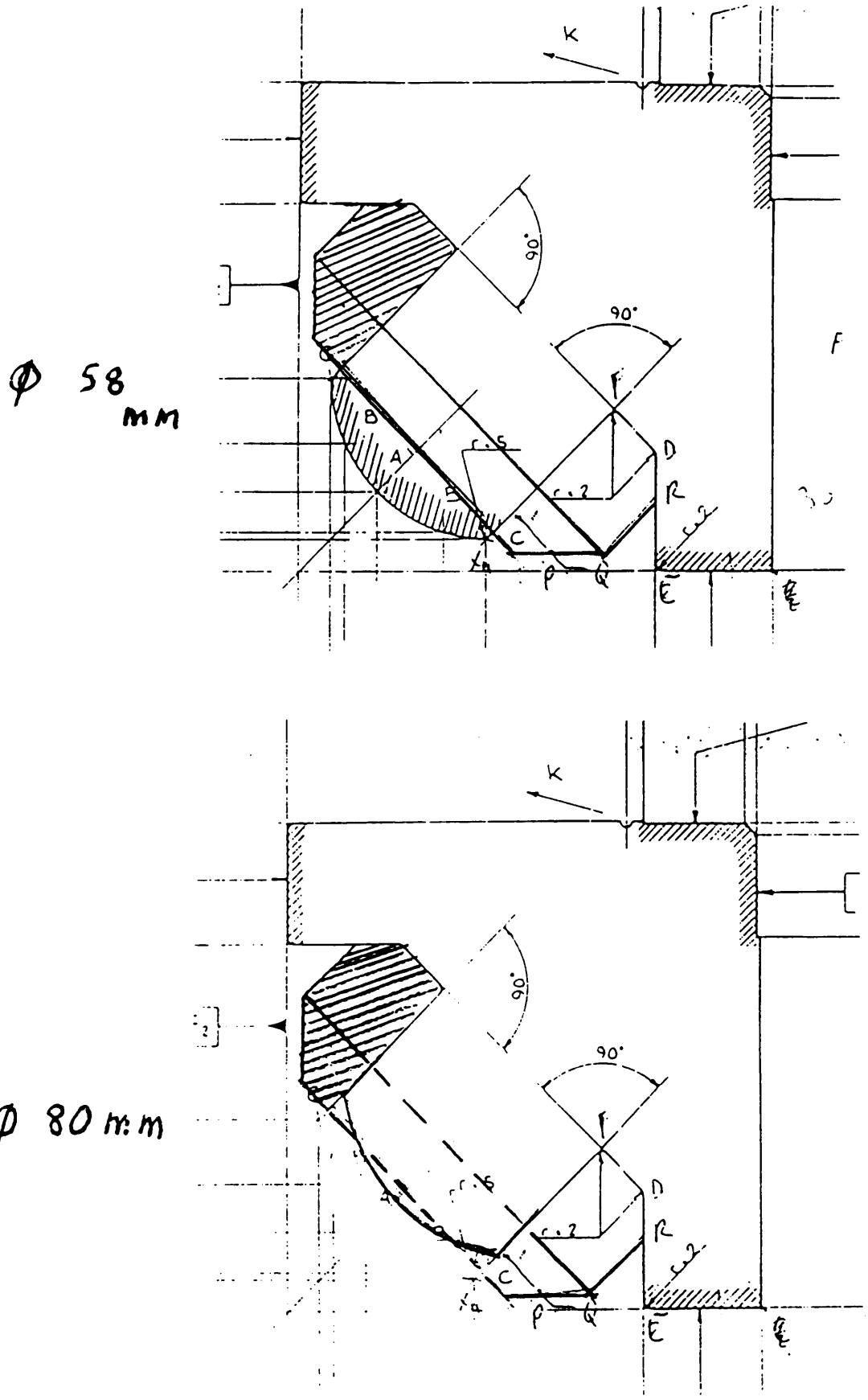

Fig. 12 Field and stray field of the 90 deg sector magnet

14-6-90 A.d

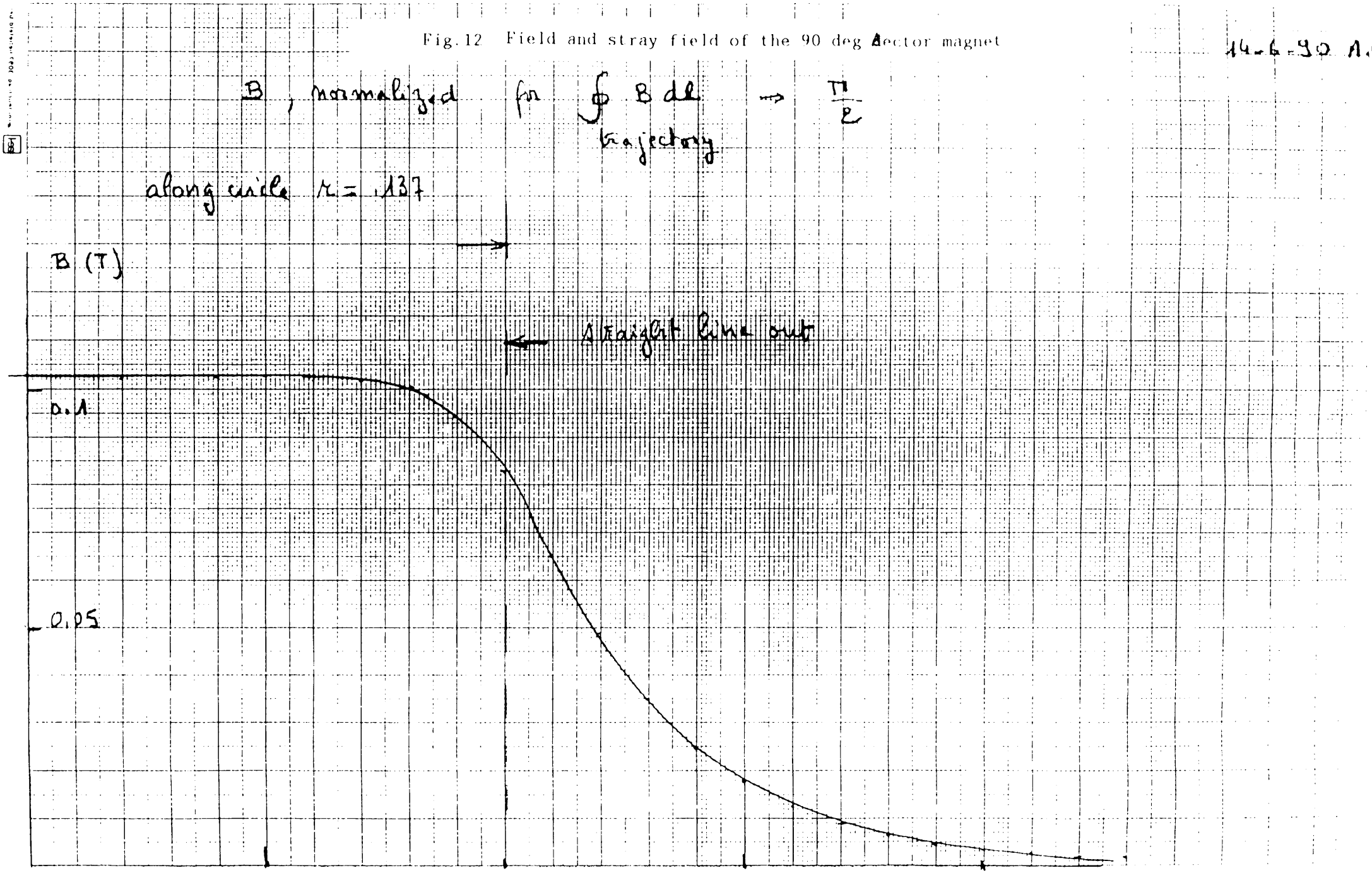

Fig. 13 Central trajectory in the fields of the 90 deg sector magnet, with indication of the vacuum chamber

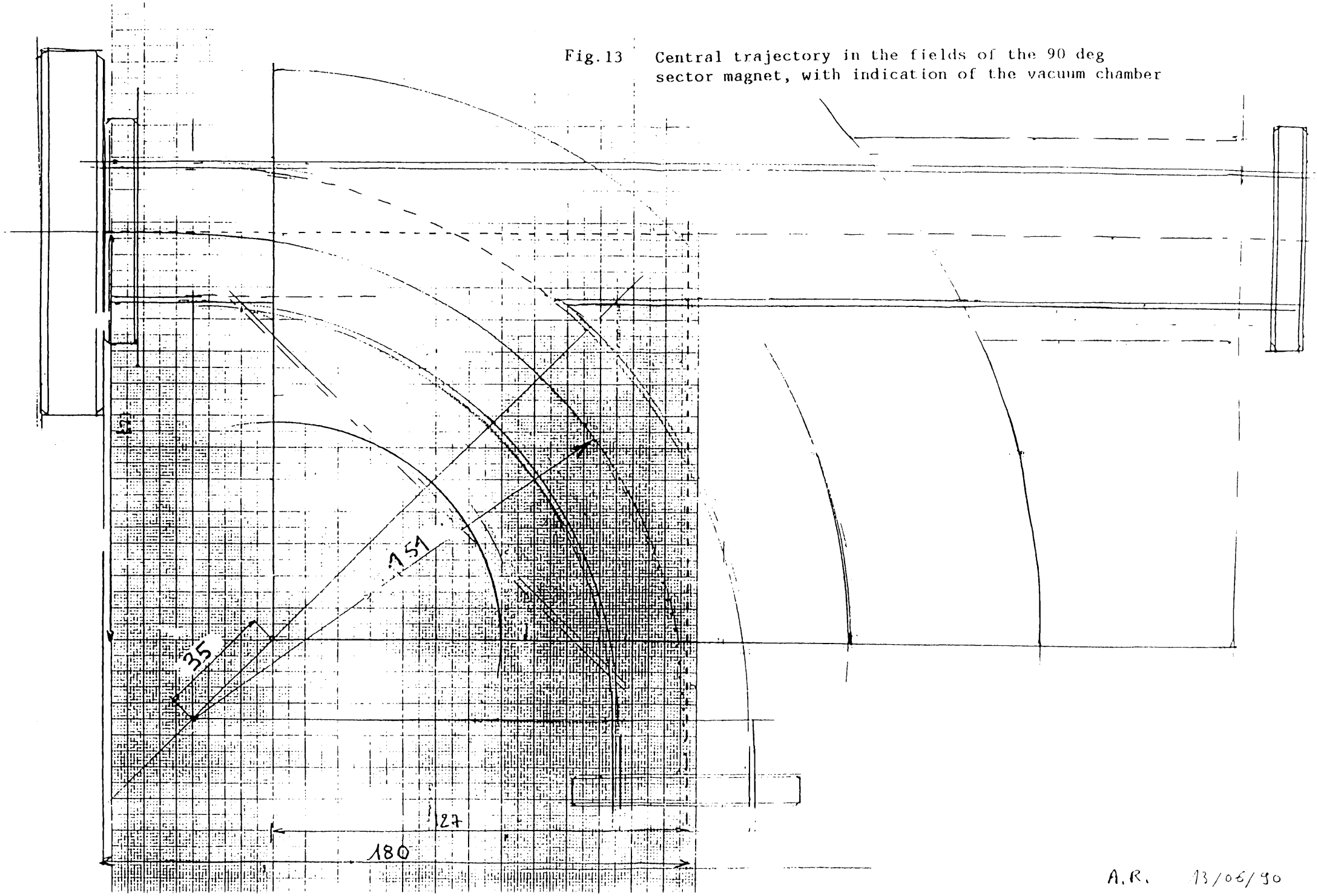

A.R. 13/06/90

Fig.14: 90 deg. sector magnet, view of the front face, above the symmetry plane

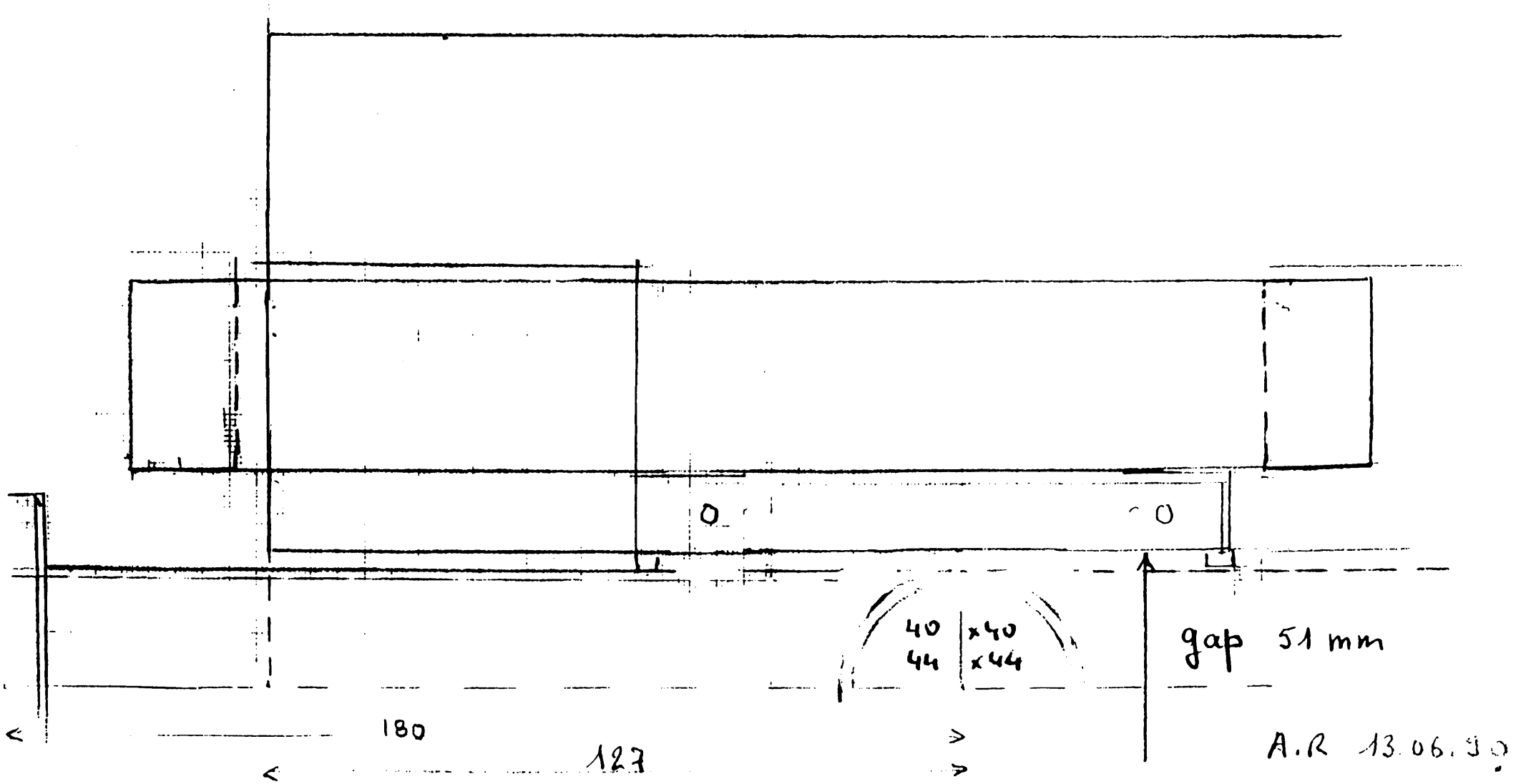

Fig. 15: ' enlarged ' CTF correction dipoles. (80/120, 120/160)
the ' normal ' dipoles are (60/100, 100/140)

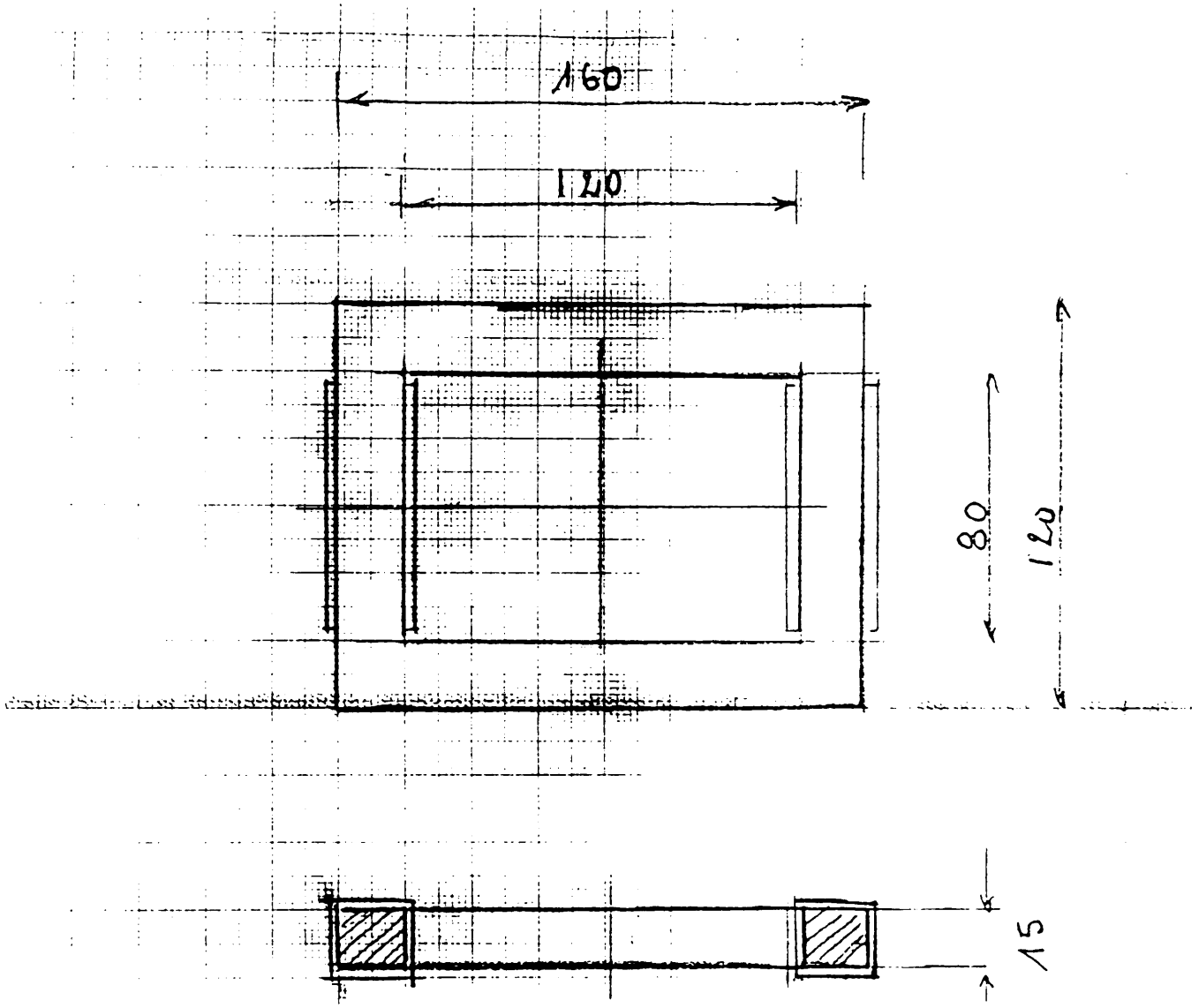

échelle 1/2